Hemodialysis Membrane Prepared from Cellulose/*N*-Methylmorpholine-*N*-oxide Solution. IV. Comparative Studies on the Surface Morphology of Membranes Prepared from *N*-Methylmorpholine-*N*-oxide and Cuprammonium Solutions

Yoshihiko Abe, Akira Mochizuki*

Research and Development Center, Terumo Corporation, 1500 Inokuchi, Nakai-machi, Aahigarakami-gun, Kanagawa 259-0151, Japan

Received 20 July 2009; accepted 25 November 2009
DOI 10.1002/app.31848
Published online 4 February 2010 in Wiley InterScience (www.interscience.wiley.com).

ABSTRACT: The surface morphology of regenerated cellulose membranes prepared by casting cellulose/*N*-methylmorpholine-*N*-oxide (NMMO) and cuprammonium solutions onto a glass plate (denoted NMMO membrane and cuprammonium membrane, respectively) were studied by using scanning electron microscopy (SEM) and atomic force microscopy (AFM). The concentration of cellulose in the casting solution was 8 wt %. The SEM images of the surfaces of both membranes indicated that they had aggregate structures formed by cellulose particles (10–150 nm in diameter). In the NMMO membrane, the glass-side surface was composed of larger particles and was rougher than the air-side surface. However, in the cuprammonium membrane there was little structural difference between air-side and glass-side surfaces. The AFM images showed that all surfaces were rough due to the cellulose particles. As for the NMMO membrane, the difference in the surface structure between the air-side and the glass-side was the same as observed by SEM. AFM also indicated that the order of the surface roughness was as follows: glass-side of NMMO membrane > air-side of NMMO membrane > air-side of cuprammonium membrane ≅ glass-side of cuprammonium membrane. On the basis of these results observed for both membranes, the reason for the difference in the performances of NMMO and cuprammonium membranes is discussed from the viewpoint of surface structure. © 2010 Wiley Periodicals, Inc. J Appl Polym Sci 116: 3040–3046, 2010

Key words: atomic force microscopy (AFM); membranes; surfaces

INTRODUCTION

Polymer membranes have largely contributed to the development of medical treatments. In particular, dialysis membranes have played a very important role in renal failure as artificial kidneys.[1,2] The regenerated cellulose membrane prepared by the cuprammonium rayon method was the first hemodialysis membrane in clinical use, and is still in use. However, it has been pointed out that the conventional cellulose membrane has two major faults in comparison with synthetic polymer membranes. One of the faults is its poor blood compatibility, represented by complement activation during extracorporeal circulation.[3–5] This problem was improved by membrane surface modification methods, such as the grafting of poly(ethylene glycol)[6,7] or the coating of vitamin E[8] on the membrane surface. The other is its low ultrafiltration rate (UFR) performance. In addition, it is said that the performance for the removal of low molecular weight proteins is not sufficient (e.g., the accumulation of β_2-microglobulin (β_2-MG; 11.8 kDa) in a patient's body could bring about amyloidosis).[9] This lower permeability is caused by the cellulose membrane structure. That is, the cellulose membrane has a homogeneous and dense structure, depending on the membrane preparation method. One of the methods to improve the poor permeability is the introduction of an asymmetric structure to it such as a synthetic polymer membrane.[10,11] Inamoto et al. studied the effect of the regeneration conditions in the cuprammonium rayon method on the membrane structure and succeeded in preparing a cellulose membrane having an asymmetric structure and high performance. Another way to obtain an asymmetric structure is to change the solvent from a cuprammonium solution to an organic solvent because it is expected that a membrane can form via a simple coagulation mechanism similar to that of synthetic polymer membranes.[12] From this viewpoint, *N*-

**Present address:* Department of Bio-Medical Engineering, Tokai University, Nishino 317, Numazu, Shizuoka 410-0395, Japan.
Correspondence to: Y. Abe (Yoshihiko_Abe@terumo.co.jp).

methylmorpholine-*N*-oxide (NMMO) is an attractive solvent because of its strong ability to dissolve cellulose, and the applications of the solvent to the manufacture of cellulosic products, such as fiber and film (the NMMO method), have been investigated.[13–15] Indeed, regenerated cellulose fiber produced by the NMMO method was industrialized,[16] and a lot of studies on the manufacturing and characterization of the fiber have been carried out.[17–19] Such studies on the NMMO method interested us, and we began to look into the feasibility of this method for preparing a hemodialysis membrane with high membrane performance. In previous articles,[20–22] for membranes prepared from a cellulose/NMMO solution (NMMO membrane), the relationships between the preparation conditions of the membrane (i.e., the cellulose concentration of the casting solution, coagulant composition, and coagulant temperature) and the membrane performance were reported. In comparison with the cuprammonium membrane, the NMMO membrane had excellent performance in regard to the UFR, diffusive solute permeability, and sieving coefficient (SC).[20] Observation by SEM under low magnification showed that both membranes apparently had the same structures, and they were classified into dense, nonporous membranes. However, the estimation of the pore structures of both membranes according to the Hagen-Poiseuille law showed that the NMMO membrane had larger pore radii and a smaller number of pores than the cuprammonium membrane.[21,22] These results led to the conclusion that the higher performances of the NMMO membrane were caused by the larger pore size. Thus, in this study, we compared the surface morphology of the NMMO membrane with that of the cuprammonium membrane by using SEM and AFM, and discuss the reason for the differences in the performance between the two types of membranes.

EXPERIMENTAL

Materials

The cellulose used was cotton linter containing over 97.5% α-cellulose, purchased from Taihei Paper Manufacture Co. (Tokyo, Japan). The viscosity of the cellulose/cupriethylenediamine solution (cellulose = 0.5 wt %) and polymerization degree of cellulose were 7.3 cP and 1180, respectively. NMMO monohydrate (containing 13.3 wt % water, melting point = 72°C) was supplied by Nippon Nyukazai Co. (Tokyo, Japan). *n*-Propyl gallate, sodium *n*-dodecyl sulfate, a 25 wt %. NH_3 aqueous solution, Na_2SO_3, $CuSO_4{\cdot}Cu(OH)_2$, NaOH, and H_2SO_4 were reagent grade, purchased from Kanto Kagaku Co. (Tokyo, Japan). *n*-Propyl gallate is one of the polyphenolic anti-oxidants and protects cellulose from oxidative decomposition.

Preparation of the membranes

As reported in previous articles,[20,21] two kinds of regenerated cellulose membranes were prepared from a cellulose/NMMO solution and from a cellulose/cuprammonium solution (denoted NMMO membrane and cuprammonium membrane, respectively). The cellulose concentration in the solution was 8 wt % in both cases. The cellulose solution was cast onto a glass plate, and the plate was immediately soaked in a coagulant bath. In the NMMO method, the coagulant used was pure water, and its temperature was 5°C. In the cuprammonium rayon method, the coagulation of cellulose was carried out in a 3.5 *N* NaOH aqueous solution at 26°C, and then regeneration was carried out in a 1 wt % H_2SO_4 aqueous solution at room temperature.

Observation of the membrane surface morphology

In observing the membrane surface, we distinguished the top and bottom surfaces of the membranes as follows:

1. Glass-side surface means the surface in contact with a glass plate when the solution was cast.
2. Air-side surface is the surface in contact with air when the solution was cast.

Preparation of the dry membrane

The as-cast wet membrane was dehydrated according to the method reported by Fukuda.[23] Briefly, the wet membrane was soaked in 50, 70, 80, 90, 95, and 99 vol % ethanol aqueous solutions and ethanol successively for 30 min each; then it was soaked in ethanol, *t*-butanol/ethanol (50/50 vol %), and *t*-butanol successively for 30 min each to substitute the alcohol with water in the membrane, after which it was freeze-dried *in vacuo* for 3 days.

SEM observation

The dry membrane was sputter-coated with platinum by a magnetron sputter (JUC-5000, JEOL, Tokyo, Japan) before observation under an SEM equipped with a field emission gun (JSM-840F, JEOL, Tokyo, Japan). The sputter-coating produced a platinum layer about 1.5 nm thick on the surface. After sputtering, the surfaces of the membrane were observed by SEM.

AFM observation

The surface morphology of the dry membrane was observed by an AFM (Probe station/Unit; SPI3800/SPA300, Seiko Instruments, Tokyo, Japan). The

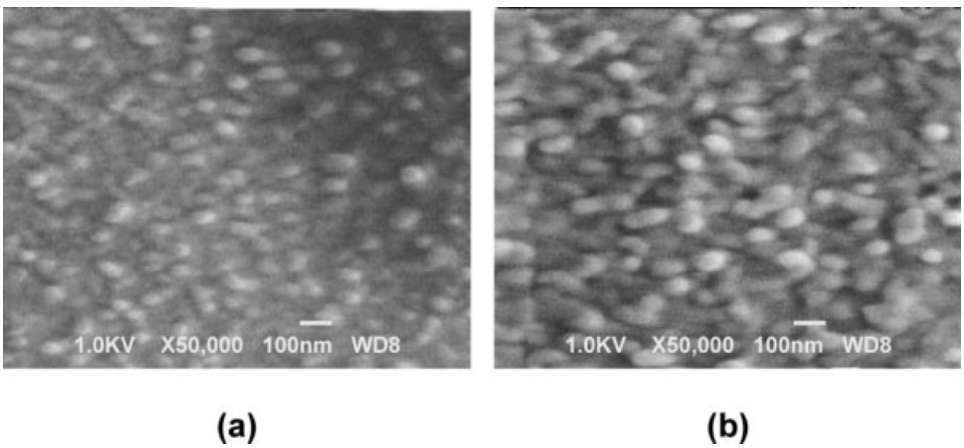

Figure 1 SEM micrographs of the surfaces of the NMMO membrane. (a) Air-side, (b) Glass-side. The bar length in all micrographs is 100 nm.

scanning was carried out at room temperature in air, using a scanner (FS-20A, Seiko Instruments, Tokyo, Japan) in dynamic force mode with a silicon cantilever tip (SI-DF20, Seiko Instruments, Tokyo, Japan). The scan speed was 0.8 Hz in a 500 × 500 nm area (x-, y- direction). The surface roughness parameters were measured by SPI3800/SPA300-dedicated software (SPIWin ver.2.31F, Seiko Instruments, Tokyo, Japan).

RESULTS AND DISCUSSION

SEM observation

We found that the performance of the NMMO membrane was higher than that of the cuprammonium membrane[20] and attempted to clarify the reason for the difference in terms of the membrane structure. SEM observation with low magnification (i.e., × 1000 × 5000) revealed that the NMMO and cuprammonium membranes had dense and nonporous structures.[21,22] These facts alone could not explain the differences in the performances between the NMMO and cuprammonium membranes. Therefore, in this study we observed the morphology of these membranes in detail by SEM with higher magnification (i.e., × 50,000) and AFM. First, the investigation by SEM is described. The results are shown in Figures 1 and 2, which are SEM micrographs of NMMO and cuprammonium membranes [Figs. 1(a) and 2(a) show the top surface (air-side) and Figs. 1(b) and 2(b) show the bottom surface (glass-side)], respectively. It is known that a cuprammonium membrane has a surface composed of numerous cellulose particles, which are nanometer-sized, formed by alkaline coagulation.[10,23,24] These pictures indicate that both membranes have aggregate structures formed by cellulose particles of which the sizes range from 10 to 150 nm. Moreover, on the NMMO membrane surfaces the particle size is larger and the surface is rougher on the glass-side than on the air-side. Meanwhile, in the cuprammonium membrane,

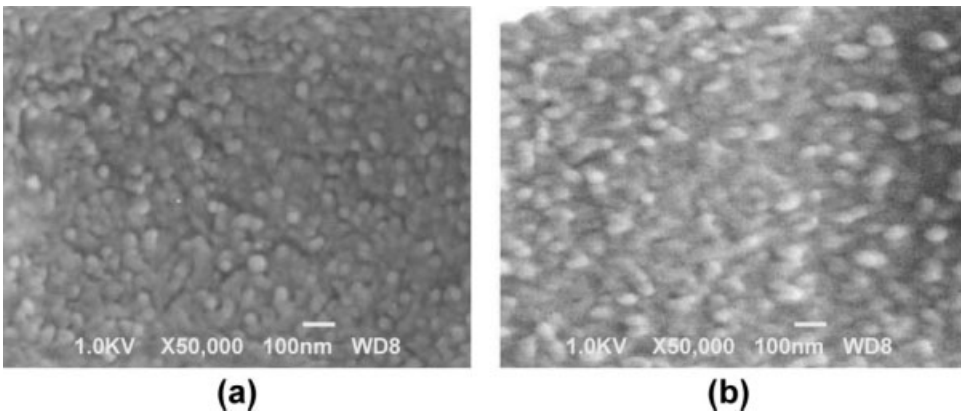

Figure 2 SEM micrographs of the surfaces of the cuprammonium membrane. (a) Air-side, (b) Glass-side. The bar length in all micrographs is 100 nm.

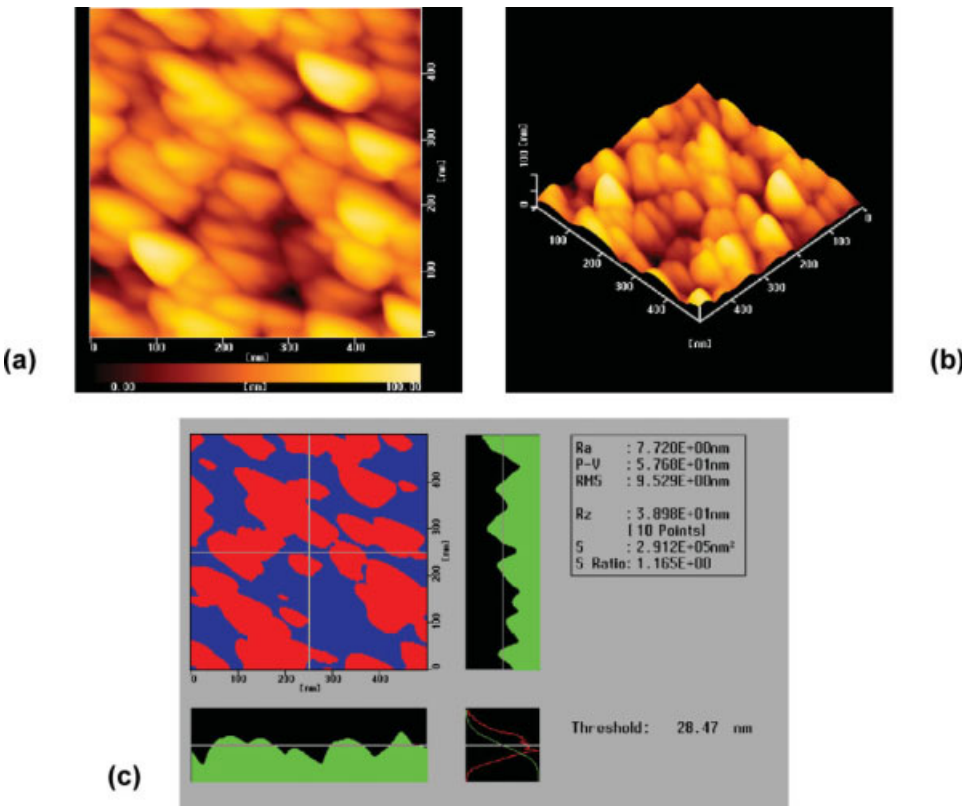

Figure 3 AFM images of the air-side surface of the NMMO membrane. (a) Top-view image (X: 500 nm × Y: 500 nm, X, Y: 100 nm per division), (b) 3D image (X: 500 nm × Y: 500 nm × Z: 100 nm, X, Y: 100 nm per division, Z: 50 nm per division), (c) Surface roughness parameters. [Color figure can be viewed in the online issue, which is available at www.interscience.wiley.com.]

the structure of the air-side surface shows little difference from the glass-side one.

Atomic force microscopic observation

Along with the development of the Atomic force microscopic (AFM) method, much research on the characterization of the surface of fibers and membranes has been carried out.[25–29] Hongo et al.[28] reported the surface morphology of various regenerated cellulose fibers by AFM.[2,9] Compared with SEM, AFM has the advantage of measuring the vertical direction. Thus, AFM measurement is expected to provide information on the 3-dimensional (3D) structural difference between NMMO and cuprammonium membranes causing the difference in permeation performance. For the NMMO membrane, AFM images of the top surface of the air-side and glass-side surfaces are shown in Figures 3 and 4. Figures 5 and 6 are images of the cuprammonium membrane. In these figures, (a) and (b) are top-view and 3D images, respectively, and (c) is result of surface roughness parameters measured by SPI3800/SPA300-dedicated software. The top-view images show that all the surfaces are rough due to the aggregation of cellulose particles and that the particle size ranges from 10 to 150 nm in diameter. These images are in good agreement with the SEM results mentioned earlier. As for the NMMO membrane, the structural difference between the air-side and the glass-side is similar to that observed by SEM. The surface roughness features are listed in Table I, which are roughness average (Ra), peak-to-valley roughness (P–V), root-mean-square (RMS), ten-point mean roughness (Rz), surface area (*S*), and ratio of *S* to scan area (*S* Ratio). For the NMMO membrane, Ra, RMS, and Rz of the glass-side surface were higher than those of the air-side, and also P–V of the glass-side is about twice as high as that of the air-side. Thus, it is clear that the glass-side surface is rougher than the air-side surface. Meanwhile, in the cuprammonium membrane, there is little difference between the air-side and the glass-side surfaces regarding Ra, RMS, and Rz, indicating that the surface roughness of both sides is the same. There is no difference between the *S* Ratio of the air-side and that of the glass-side in each membrane (1.165 and 1.154 for NMMO membrane, 1.093 and 1.078 for cuprammonium membrane, respectively), although the NMMO membrane has a higher *S* Ratio than the cuprammonium membrane. This *S* Ratio result corresponds to the roughness features mentioned

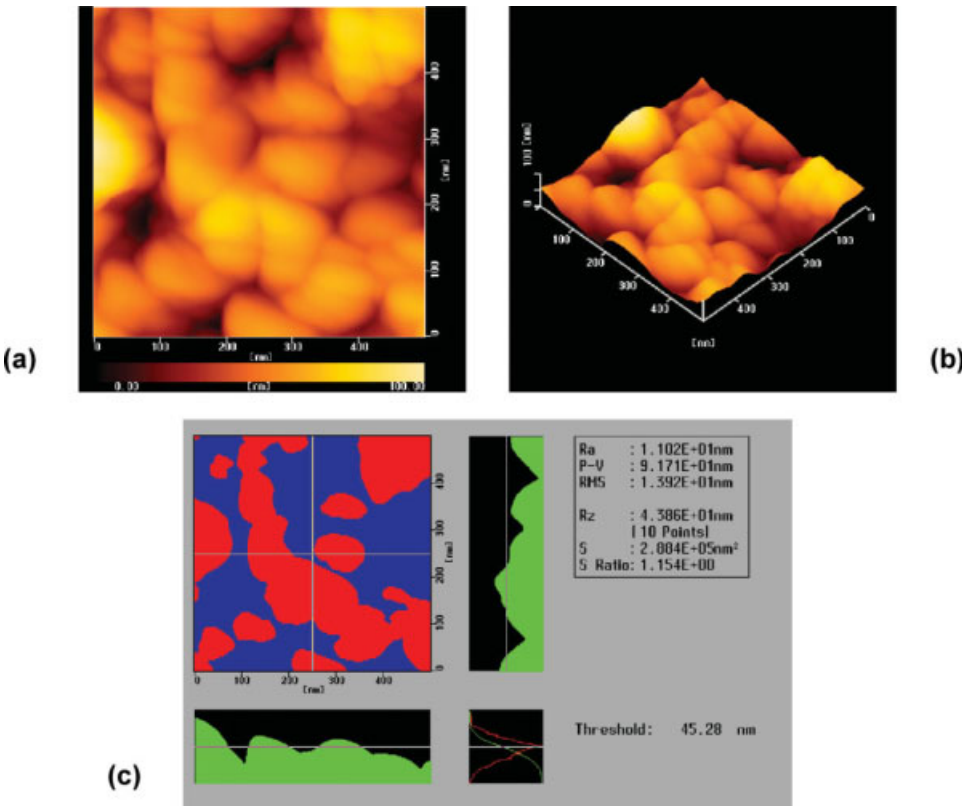

Figure 4 AFM images of the glass-side surface of the NMMO membrane. (a) Top-view image (X: 500 nm × Y: 500 nm, X, Y: 100 nm per division), (b) 3D image (X: 500 nm × Y: 500 nm × Z: 100 nm, X, Y: 100 nm per division, Z: 50 nm per division), (c) Surface roughness parameters. [Color figure can be viewed in the online issue, which is available at www.interscience.wiley.com.]

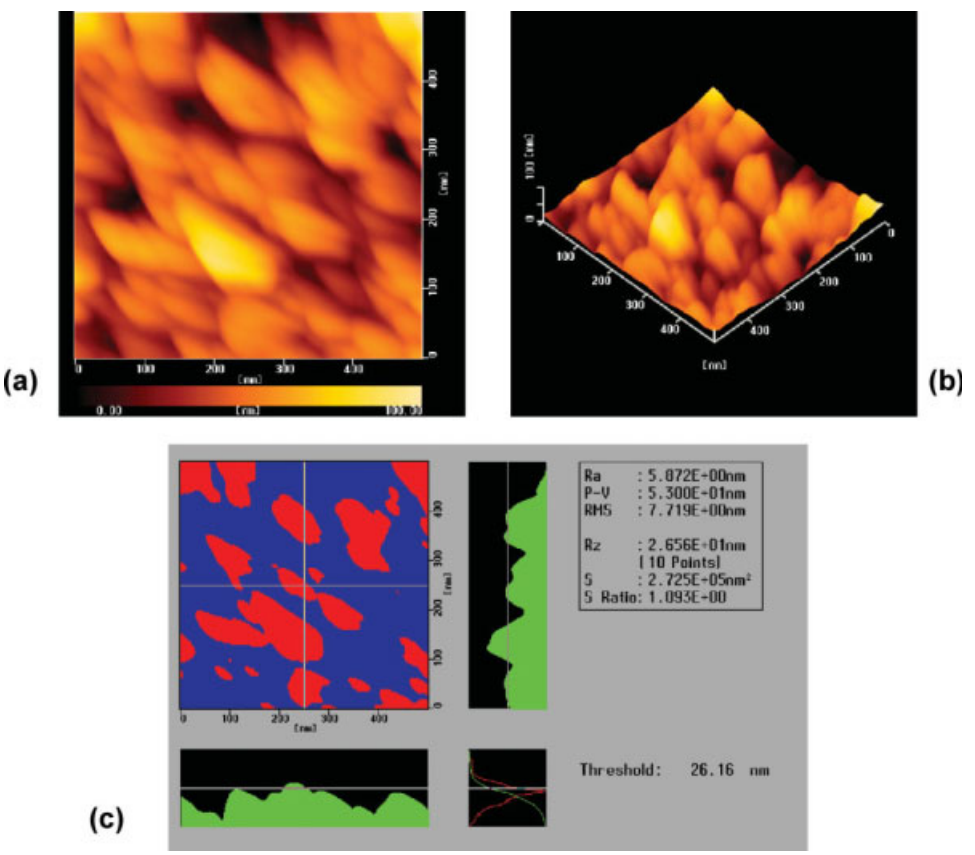

Figure 5 AFM images of the air-side surface of the cuprammonium membrane. (a) Top-view image (X: 500 nm × Y: 500 nm, X, Y: 100 nm per division), (b) 3D image (X: 500 nm × Y: 500 nm × Z: 100 nm, X, Y: 100 nm per division, Z: 50 nm per division), (c) Surface roughness parameters. [Color figure can be viewed in the online issue, which is available at www.interscience.wiley.com.]

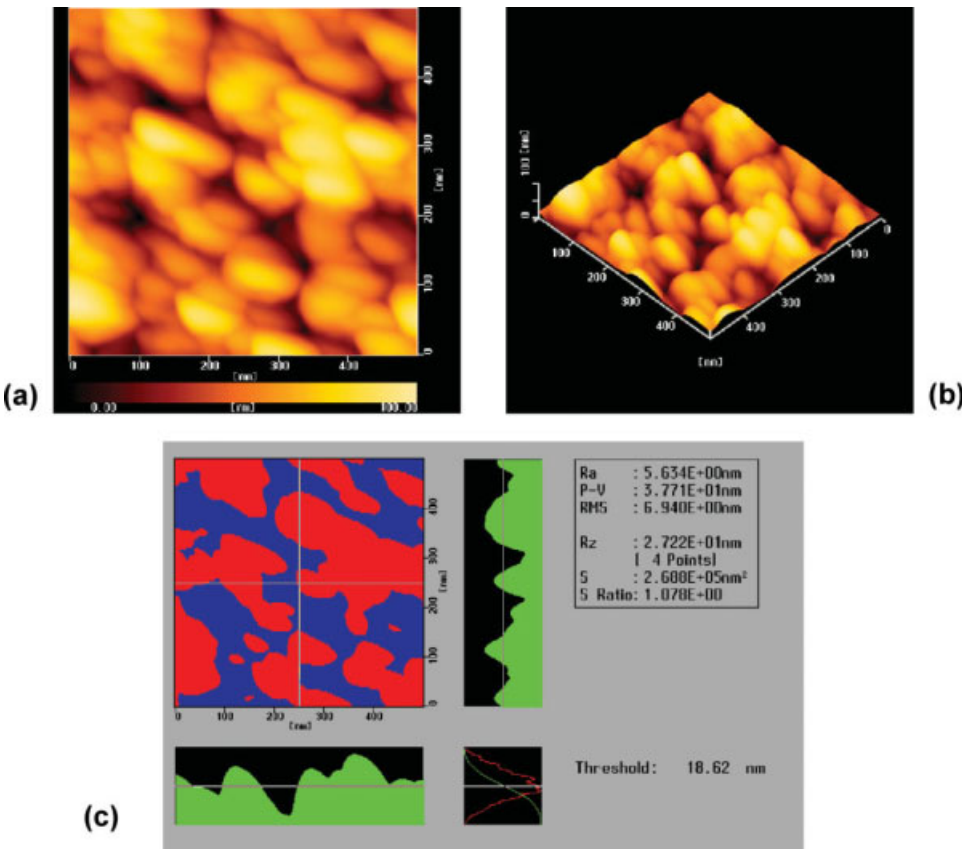

Figure 6 AFM images of the glass-side surface of the cuprammonium membrane. (a) Top-view image (X: 500 nm × Y: 500 nm, X, Y: 100 nm per division), (b) 3D image (X: 500 nm × Y: 500 nm × Z: 100 nm, X, Y: 100 nm per division, Z: 50 nm per division), (c) Surface roughness parameters. [Color figure can be viewed in the online issue, which is available at www.interscience.wiley.com.]

earlier – that is, the surface of the NMMO membrane is rough compared with that of the cuprammonium membrane. It is concluded that the order of the surface roughness is glass-side of NMMO membrane > air-side of NMMO membrane > air-side of cuprammonium membrane ≅ glass-side of cuprammonium membrane. This result is in good agreement with the SEM images mentioned earlier.

As the degree of surface roughness depends on the size of the cellulose particle, the larger the cellulose particle size is, the higher the surface roughness is. The roughness or the particle size is determined by the coagulation process, and the difference in the roughness between the air-side and glass-side surface is explained as follows. NMMO dissolves cellulose directly without the formation of a cellulose complex or its derivatives, whereas a cuprammonium hydroxide solution dissolves cellulose by forming a complex with cellulose. Thus, cellulose can easily be regenerated from an NMMO solution via a simple mechanism called phase-inversion. In the coagulation process, NMMO is gradually replaced by water from the air-side to the glass-side surfaces and, at the same time, the cellulose particles are formed in the casting solution and aggregated from the air-side to the glass-side. The replacement of NMMO with water is slow when the distance from the air-side surface is longer, resulting in the slow coagulation and the promotion of particle

TABLE I
Roughness of Membrane Surface Analyzed by AFM

	Membrane			
	NMMO		Cuprammonium	
Parameter*	Air-side	Glass-side	Air-side	Glass-side
Ra (nm)	7.72	11.02	5.87	5.63
P-V (nm)	57.68	91.71	53.00	37.71
RMS (nm)	9.53	13.92	7.72	6.94
Rz (nm)	38.98	43.86	26.56	27.22
S (nm^2)	291,200	288,400	272,500	268,800
S Ratio	1.165	1.154	1.093	1.078

* Ra, roughness average; P-V, peak-to-valley roughness; RMS, root-mean-square; Rz, ten-point mean roughness; S, surface area; S Ratio, surface area (S)/scan area (250,000 nm^2). The surface with S Ratio = 1 is completely flat and smooth, and the surface roughness increases with the increasing the S Ratio greater 1.

growth. Thus, the particle size of the glass-side surface is larger than that of the air-side one. On the contrary, in the cuprammonium rayon method the coagulation/regeneration process is very complicated.[30] This process involves coagulation with NaOH for forming cellulose and an Na^+ complex in the Normann reaction,[31] and regeneration is completed by soaking in an acid solution. The cellulose particles are homogeneously formed in the casting solution on any side by the Normann reaction, resulting in little difference in the particle sizes between the air-side and the glass-side surfaces. The reason for the larger particle size in the NMMO membrane than in the cuprammonium membrane is not yet clear.

As mentioned earlier, we reported that the NMMO membrane had high performance in regard to UFR, SC, and solute permeability,[20] and analysis by the Hagen-Poiseuille law suggested that the NMMO membrane had large pores in comparison with those of the cuprammonium membrane. It is very easy to predict that the larger particles form larger pores and a smaller number of pores in a membrane. This is supported by the report that the surface roughness of the cellulose membrane increased with an increase in UFR.[23] The results obtained in this work and the earlier-mentioned results on membrane performance and the semi-empirical pore structure lead to the conclusion that the high performance of the NMMO membrane is due to the larger cellulose particle which forms the membrane structure.

CONCLUSIONS

The surface morphology of regenerated cellulose membranes prepared from solutions of NMMO and cuprammonium were studied by SEM and AFM. The SEM images indicated that both membrane surfaces had aggregate structures formed by cellulose particles. In the NMMO membrane, the glass-side surface had larger particles and was rougher than the air-side surface. However, in the cuprammonium membrane, the glass-side surface had a similar structure to the air-side surface. The AFM images showed that all surfaces were rough due to the aggregation of cellulose particles. As for the NMMO membrane, the structural difference between the air-side and the glass-side was similar to that observed by SEM. The order of the surface roughness was glass-side of NMMO membrane $>$ air-side of NMMO membrane $>$ air-side of cuprammonium membrane $\cong$ glass-side of cuprammonium membrane. On the basis of SEM and AFM results, we concluded that the high performance of the NMMO membrane was due to the large size of the cellulose particles.

The authors thank Dr. Takeshi Ito and Mr. Masahiko Mitsuhashi of Kanagawa Industrial Technology Center, (Kanagawa, Japan) for technical support in the use of the AFM, and for useful discussions and advice in regard to analyzing the features of the membrane surface roughness.

References

1. Ward, R. A.; Feldhoff, P. W.; Klein, E. In Materials Science of Synthetic Membranes; Lloyd, D. R., Ed.; American Chemical Society: Washington, DC, 1985; pp 99–118.
2. Klein, E.; Ward, R. A.; Lacey, R. E. In Handbook of Separation Process Technology; Rousseau, R. W., Ed.; Wiley: New York, NY, 1987; pp 954–981.
3. Craddock, P. R.; Fehr, J.; Dalmasso, A. P.; Brigham, K. L.; Jacob, H. S. J Clin Invest 1977, 59, 879.
4. Hakim, R. M.; Breillatt, J.; Lazarus, J. M.; Port, F. K. N Engl J Med 1984, 311, 878.
5. Cheung, A. K.; Wilcox, L. A.; Janatova, J. Kidney Int 1990, 37, 1055.
6. Kishida, A.; Mishima, K.; Corretge, E.; Konishi, H.; Ikada, Y. Biomaterials 1992, 13, 113.
7. Kanamori, T.; Sakai, K.; Fukuda, M.; Yamashita, Y. J Appl Polym Sci 1995, 55, 1601.
8. Sasaki, M.; Hosoya, T.; Watanabe, H.; Tsukamoto, H.; Saruhashi, M. Maku (Membrane) 1994, 19, 400.
9. Gejyo, F.; Yamada, T.; Odani, S. Biochem Biophys Res Commun 1985, 129, 701.
10. Inamoto, M.; Miyamoto, I.; Hongo, T.; Iwata, M.; Okajima, K. Polym J 1996, 28, 507.
11. Hongo, T.; Inamoto, M.; Iweata, M.; Matsui, T.; Okajima, K. J Appl Polym Sci 1999, 72, 1669.
12. Matsuda, M.; Kamizawa, C.; Kobayashi, R. Maku (Membrane) 1987, 12, 49.
13. Chanzy, H.; Peguy, A.; Chaunis, S.; Monzie, P. J Polym Sci: Polym Phys Ed 1980, 18, 1137.
14. Loubinoux, D.; Chaunis, S. Lenzinger Ber 1985, 59, 105.
15. Bochek, A. M.; Petropavlovskii, G. A.; Kallistov, O. V. Cellul Chem Technol 1990, 24, 727.
16. Eichinger, D.; Eibl, M. Lenzinger Ber 1995, 75, 41.
17. Cho, S.; Kamata, M.; Hayami, A.; Shibayama, M.; Nomura, S. Sen' Gakkash 1995, 51, 422.
18. Mortimer, S. A.; Peguy, A. A.; Ball, R. C. Cellul Chem Technol 1996, 30, 251.
19. Weigel, P.; Fink, H. P.; Walenta, E.; Ganster, J.; Remde, H. Cellul Chem Technol 1997, 31, 321.
20. Abe, Y.; Mochizuki, A. J Appl Polym Sci 2002, 84, 2302.
21. Abe, Y.; Mochizuki, A. J Appl Polym Sci 2003, 89, 333.
22. Abe, Y.; Mochizuki, A. J Appl Polym Sci 2003, 89, 1671.
23. Fukuda, M.; Miyazaki, M.; Hiyoshi, T.; Iwata, M.; Hongou, T. J Appl Polym Sci 1999, 72, 1249.
24. Kamide, K.; Manabe, S. Materials Science of Synthetic Membranes; Lloyd, D. R., Ed.; American Chemical Society: Washington, DC, 1985; pp 197–228.
25. Fu, X. Y.; Sotani, T.; Matsuyama, H. Desalination 2008, 233, 10.
26. Khulbe, K. C.; Hamad, F.; Feng, C.; Matsuura, T.; Khayet, M. Desalination 2004, 161, 259.
27. Zeng, Y.; Wang, Z.; Wan, L.; Shi, Y.; Chen, G.; Bai, C. J Appl Polym Sci 2003, 88, 1328.
28. Hongo, T.; Yamane, C.; Saito, M. Sen' Gakkash 1998, 54, 511.
29. Zhang, Y.; Shao, H.; Hu, X. J Appl Polym Sci 2002, 86, 3389.
30. Fushimi, F.; Watanabe, T.; Hiyoshi, T.; Yamashita, Y.; Osakai, T. J Appl Polym Sci 1996, 59, 15.
31. Normann, W. Chem Ztg 1906, 30, 584.